Supplemental material to this article can be found at:
http://dmd.aspetjournals.org/content/suppl/2024/11/08/dmd.124.001819.DC1
1521-009X/52/12/1396–1406$35.00
DRUG METABOLISM AND DISPOSITION
dx.doi.org/10.1124/dmd.124.001819
Drug Metab Dispos 52:1396–1406, December 2024

Characterization of Nonclinical Drug Metabolism and Pharmacokinetic Properties of Phosphorodiamidate Morpholino Oligonucleotides, a Novel Drug Class for Duchenne Muscular Dystrophy[S]

Andrew K.L. Goey, Marie Claire Mukashyaka, Yogesh Patel, Louise R. Rodino-Klapac, and Lilly East

Sarepta Therapeutics, Inc., Cambridge, Massachusetts

Received June 18, 2024; accepted September 11, 2024

ABSTRACT

Eteplirsen, golodirsen, and casimersen are phosphorodiamidate morpholino oligomers (PMOs) that are approved in the United States for the treatment of patients with Duchenne muscular dystrophy (DMD) with mutations in the *DMD* gene that are amenable to exon 51, 53, and 45 skipping, respectively. Here we report a series of in vivo and in vitro studies characterizing the drug metabolism and pharmacokinetic (DMPK) properties of these three PMOs. Following a single intravenous dose, plasma exposure was consistent for all three PMOs in mouse, rat, and nonhuman primate (NHP), and plasma half-lives were similar for eteplirsen (2.0–4.1 h) and golodirsen (2.1–8.7 h) across species and more variable for casimersen (3.2–18.1 h). Plasma protein binding was low (<40%) for all three PMOs in mouse, rat, NHP, and human and was largely concentration independent. In the *mdx* mouse model of DMD, following a single intravenous injection, extensive biodistribution was observed in the target skeletal muscle tissues and the kidney for all three PMOs; consistent with the latter finding, the predominant route of elimination was renal. In vitro studies using liver microsomes showed no evidence of hepatic metabolism, and none of the PMOs were identified as inhibitors or inducers of the human cytochrome P450 enzymes or membrane drug transporters tested at clinically relevant concentrations. These findings suggest that key DMPK features are consistent for eteplirsen, golodirsen, and casimersen and provide evidence for the concept of a PMO drug class with potential application to novel exon-skipping drug candidates.

SIGNIFICANCE STATEMENT

The PMOs eteplirsen, golodirsen, and casimersen share similar absorption, distribution, metabolism, and excretion and DMPK properties, which provides evidence for the concept of a PMO treatment class. A PMO drug class may support a platform approach to enhance understanding of the pharmacokinetic and pharmacodynamic behavior of these molecules. The grouping of novel agent series into platforms could be beneficial in the development of drug candidates for populations in which traditional clinical trials are not feasible.

Introduction

Duchenne muscular dystrophy (DMD) is an X-linked recessive neuromuscular disorder attributable to mutations in *DMD*, the gene encoding dystrophin protein. These mutations result in the absence or insufficient levels of functional dystrophin protein with consequential muscle degeneration and necrosis (Bushby et al., 2010; Duan et al., 2021). DMD is characterized by progressive and irreversible muscle damage that is ongoing at birth and results in muscular weakness, delays in motor function, loss of ambulation, impairment of respiration, and cardiomyopathy (Bushby et al., 2010; Nascimento Osorio et al., 2019). Premature death as a result of cardiac or respiratory failure usually occurs starting in the late teens or 20s (Bushby et al., 2010; Duan et al., 2021).

Treatment of DMD is primarily focused on managing disease symptoms with physiotherapy, corticosteroids, cardiac medications, and ventilation support (Bushby et al., 2010; Duan et al., 2021). A microdystrophin gene therapy, delandistrogene moxeparvovec, is indicated for the treatment of DMD in patients aged 4 or older with a confirmed mutation in the *DMD* gene (Elevidys, 2024). Although corticosteroids have been shown to maintain muscle strength and function, associated side effects include increased risk of bone fractures, behavioral changes, and weight gain (Bello et al., 2015; Guglieri et al., 2022). Burden of care associated with treatment of DMD can significantly impact patient and caregiver quality of life (Duan et al., 2021; Landfeldt et al., 2018).

This study was funded by Sarepta Therapeutics, Inc.

A.K.L.G., Y.P., L.R.R.-K., and L.E. are employees of Sarepta Therapeutics, Inc. and may own stock/options in the company. M.C.M. was an employee of Sarepta Therapeutics, Inc. at the time of manuscript preparation and is currently employed at Zenas BioPharma.

dx.doi.org/10.1124/dmd.124.001819.

[S] This article has supplemental material available at dmd.aspetjournals.org.

ABBREVIATIONS: ADME, absorption, distribution, metabolism, and excretion; AhR, aryl hydrocarbon receptor; AUC, area under the concentration–time curve; BCRP, breast cancer resistance protein; BSEP, bile salt export pump; CYP, cytochrome P450; DMD, Duchenne muscular dystrophy; DMPK, drug metabolism and pharmacokinetics; FDA, Food and Drug Administration; HLMs, human liver microsomes; IV, intravenous; Ki, inhibition constant; LC-MS/MS, liquid chromatography coupled with tandem mass spectrometry; LLOQ, lower limit of quantitation; LSC, liquid scintillation counting; MATE, multidrug and toxin extrusion; MRP2, multidrug resistance protein 2; NADPH, nicotinamide adenine dinucleotide phosphate; NHP, nonhuman primate; OAT, organic anion transporter; OATP, organic anion transporting polypeptide; OCT, organic cation transporter; P-gp, P-glycoprotein; PK, pharmacokinetic; PMO, phosphorodiamidate morpholino oligomer; $t_{1/2}$, elimination half-life.

Given that most *DMD* gene mutations cluster in the hotspot region of exons 45–55 (Aartsma-Rus et al., 2009), a substantial proportion (~43%) of *DMD* mutations are likely amenable to exon-skipping antisense oligonucleotides. The use of targeted antisense oligonucleotides to skip specific exons within the *DMD* gene has been an effective approach for the treatment of patients with DMD (Popplewell et al., 2009; Mendell et al., 2013). Exon skipping restores the reading frame by splicing out the exon bordering the mutated region in the targeted pre-mRNA, allowing the production of an internally shortened but functional dystrophin protein (Aartsma-Rus et al., 2009). Phosphorodiamidate morpholino oligomers (PMOs) are exon-skipping agents with strong sequence-specific binding to RNA targets (Popplewell et al., 2009; Kole et al., 2012). PMOs have demonstrated favorable and predictable safety profiles in preclinical and clinical evaluations (Sazani et al., 2010, 2011a,b; Mendell et al., 2013; Carver et al., 2016; Clemens et al., 2020; Frank et al., 2020; Wagner et al., 2021), and they have been shown to attenuate key disease milestones, including ambulatory and pulmonary decline (Mendell et al., 2016, 2021; Servais et al., 2022) and survival (Iff et al., 2024) when compared with matched natural history controls. Eteplirsen was the first PMO to be approved under accelerated approval by the US Food and Drug Administration (FDA) for the treatment of patients with *DMD* mutations amenable to exon 51 skipping (Exondys 51, 2022). Subsequently, other PMOs were approved under accelerated approval by the US FDA for the treatment of patients with *DMD* mutations amenable to exon 53 (golodirsen, viltolarsen) and exon 45 (casimersen) skipping (Viltepso, 2021; Vyondys 53, 2021; Amondys 45, 2023).

Here we report findings from animals [mice, rats, and nonhuman primates (NHPs)] and in vitro systems (hepatic microsomes, human hepatocytes, and human transporter proteins) intended to characterize the absorption, distribution, metabolism, and excretion (ADME) and drug metabolism and pharmacokinetic (DMPK) properties of PMOs, specifically focusing on eteplirsen, golodirsen, and casimersen, that guided the clinical development and clinical pharmacology evaluations for the treatment of DMD and further enhanced the understanding of PMOs as a drug class. The molecular structures of these three PMOs are shown (Fig. 1), and an overview of their molecular formulas and molecular weights is provided (Table 1).

Materials and Methods

Study Design

A series of animal and in vitro studies was conducted during the development of eteplirsen, golodirsen, and casimersen to evaluate their ADME and DMPK properties. Animal studies complied with all local and national regulatory principles and guidelines for the use and care of laboratory animals. Procedures were in compliance with the Animal Welfare Act, the Office of Laboratory Animal Welfare, and the Guide for the Care and Use of Laboratory Animals. In vitro and in vivo studies were conducted by Covance Laboratories Inc. (Madison, WI, USA) and Charles River Laboratories Preclinical Services (Montreal, QC, Canada). All studies were conducted and analyzed according to a predefined protocol.

Plasma Pharmacokinetic Properties

Plasma pharmacokinetic (PK) properties of eteplirsen, golodirsen, and casimersen were assessed in mice, rats, and NHPs.

In mice, eteplirsen was administered to male CByB6F1 mice by a single intravenous (IV) bolus injection into the tail vein at a dose of 100, 300, 600, or 960 mg/kg ($n = 3$ animals per dose group per timepoint). Blood was collected at 0.083, 0.5, 1, 4, 8, and 24 h postdose from the retro-orbital sinus following CO_2 anesthesia. The plasma PK properties of golodirsen and casimersen were assessed in male C57BL/6NCrl mice following a single dose of 12, 120, or 960 mg/kg ($n = 3$ animals per dose group per timepoint for each PMO) administered by IV bolus injection into the caudal (golodirsen) or tail vein (casimersen). This dose range is inclusive of the clinically approved dose of 30 mg/kg. Blood was collected at 0.083, 0.25, and 0.5 h postdose and approximately 1, 2, 4, 8, 24, 36, and 48 h postdose from the abdominal aorta (golodirsen) or via cardiac puncture (casimersen) following isoflurane anesthesia.

In rats, plasma PK properties of all three PMOs were assessed in (14 days postpartum) male Sprague–Dawley rats after a single dose of 100, 300, or 900 mg/kg ($n = 4$ per dose group per timepoint for each PMO), administered by IV injection into the tail vein. Blood was collected via the abdominal aorta following isoflurane anesthesia 0.083, 0.25, 0.5, 1, 3, 8, and 24 h after dosing. Additional blood collection occurred at 36 and 48 h postdose for golodirsen and casimersen.

Plasma PK properties of all three PMOs were also assessed in mature male cynomolgus monkeys (NHPs) after a single dose of 5, 40, or 320 mg/kg ($n = 8$ per dose group for eteplirsen and $n = 9$ per dose group for golodirsen and casimersen), administered by bolus IV injection via the saphenous vein. Blood samples were collected via femoral or saphenous vein at approximately 0.25, 0.5, 1, 2, 4, 12, and 36 h postdose; the additional timepoint of 48 h was assessed for golodirsen and casimersen.

Concentrations of eteplirsen were measured using a validated high-performance liquid chromatography with fluorescence detection assay [lower limit of quantitation (LLOQ): 10 ng/mL] for mouse and rat plasma samples or a validated anion exchange high-performance liquid chromatography method with fluorescence probe hybridization (LLOQ: 10 ng/mL) for NHP plasma samples (BASi, McMinnville, OR, USA). Golodirsen and casimersen were quantitated in mouse, rat, and NHP plasma using a validated liquid chromatography coupled with tandem mass spectrometry (LC-MS/MS; LLOQ: 10 ng/mL for golodirsen and casimersen) assay at Tandem Laboratories (Salt Lake City, UT, USA) (Supplemental Methods).

PK parameters were estimated by WinNonlin software (Certara, Princeton, NJ, USA) using a noncompartmental approach and presented using descriptive statistics. PK parameters included the back-extrapolated concentration at time zero, elimination half-life ($t_{1/2}$), area under the concentration–time curve (AUC) from time zero to the last quantifiable timepoint, AUC from time zero to infinity, total body clearance, and volume of distribution or volume of distribution at steady-state. Nominal sampling times and doses were used. Concentration values below the lower limit of quantitation were assigned a value of zero.

Plasma Protein Binding

Plasma protein binding of ^{14}C-radiolabeled PMOs was assessed in vitro in CD-1 mice, Sprague–Dawley rats, NHPs, and human samples. K_2EDTA-coagulated plasma samples for each species were purchased from Bioreclamation, LLC (Westbury, NY, USA). Animal samples comprised pooled plasma obtained from at least three male animals. Human samples comprised pooled plasma obtained from three males who had reportedly not taken any medication in the previous seven days. Nominal concentrations of PMOs at 8, 24, 80, 240, and 800 μg/mL were assessed to encompass a wide range of doses inclusive of clinically relevant concentrations. The extent of binding was assessed via ultrafiltration using filter plates (Millipore Corporation, Billerica, MA, USA) with semipermeable membranes and a molecular weight of approximately 30,000 Da. Samples were centrifuged at 37°C and 2000 × g for 30 minutes. All determinations were performed in triplicate.

Distribution and Excretion in a DMD Mouse Model

Radiolabeled mass balance studies to evaluate PMO distribution and excretion were performed in male *mdx* mice (C57BL/10ScSn-*DMD*^{mdx}; stock #001801) obtained from Jackson Laboratory (Bar Harbor, ME, USA) (Bulfield et al., 1984; Ryder-Cook et al., 1988; Sicinski et al., 1989). These mice carry a point mutation in exon 23 of the *DMD* gene, which prevents expression of dystrophin. A single IV bolus dose of 120 mg/kg ^{14}C-radiolabeled PMOs was administered via tail vein; the dose was formulated to result in a radioactivity level of 300 μCi/kg of animal weight. Concentrations of radioactivity in plasma and tissues were determined by liquid scintillation counting using a 2900TR liquid scintillation counter (Perkin Elmer, Shelton, CT, USA).

Tissue Biodistribution. After the single IV dose of PMO, blood samples were collected from three mice at each of the following timepoints after sacrifice: 0.083, 0.25, 0.5, 1, 2, 4, 8, 24, 48, 72, 96, 120, and 144 h postdose. Tissue from the diaphragm, biceps brachii, tibialis anterior, biceps femoris, quadriceps, brain, heart, and kidneys were collected at 0.25, 1, 4, 8, 24, 48, 96, 120, and 144 h postdose. Quantitative whole-body autoradiography was conducted on one animal per timepoint killed at 4, 24, 72, 120, 336, and 1344 h postdose to examine

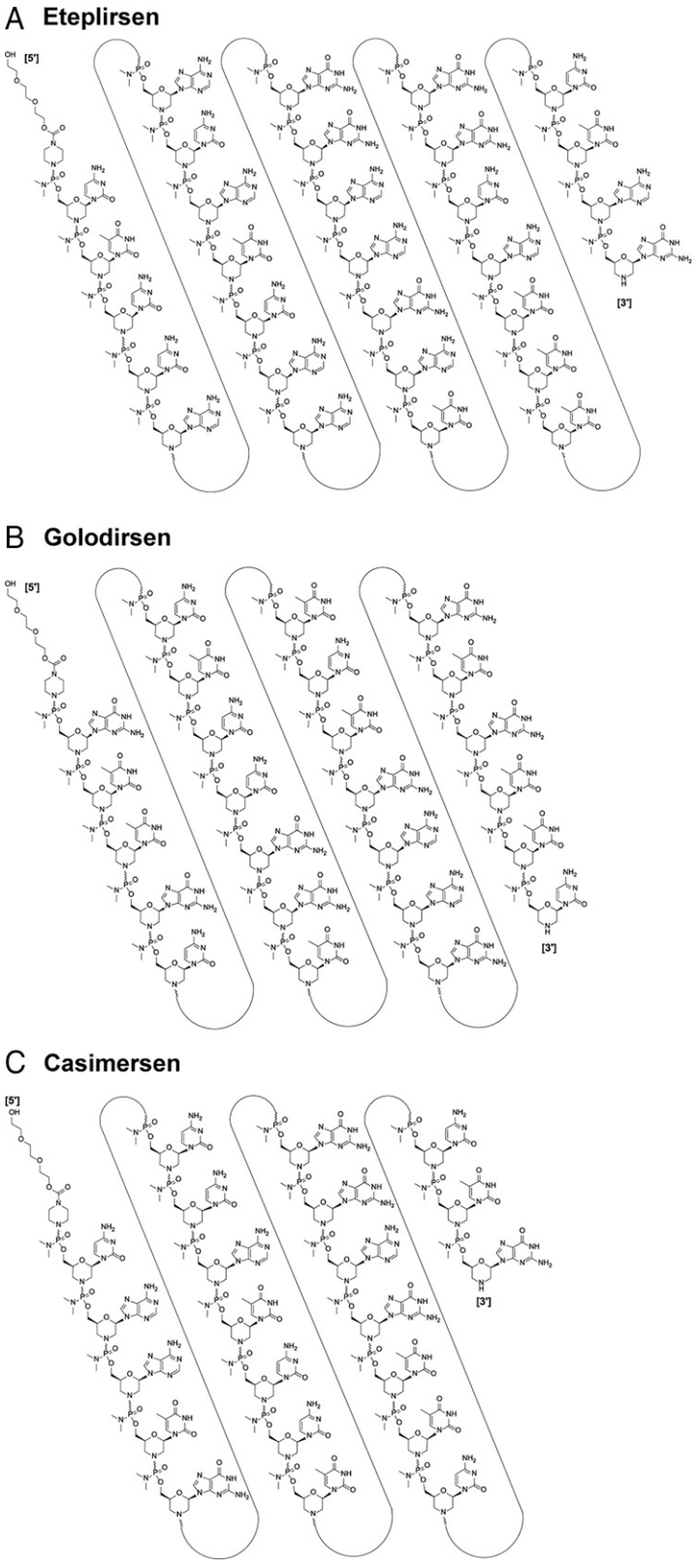

Fig. 1. Molecular structures of eteplirsen (A), golodirsen (B), and casimersen (C).

tissue distribution. Tissue sections (40-μm thickness) were collected at six levels of interest (sagittal plane), mounted, then wrapped with Mylar film and exposed on phosphorimaging screens for 4 days, along with blood standards for calibration of the image analysis software. Exposed screens were scanned using a Storm 860 Molecular Imager (Molecular Dynamics) for eteplirsen or Typhoon laser scanner (Cytiva, Marlborough, MA, USA) for golodirsen and casimersen. A calibrated standard curve was created by sampling image data using MCID Analysis software (InterFocus Imaging Ltd., Cambridge, UK). Tissue concentrations were calculated from each standard curve as nanocuries/g and converted to ng equivalents/g based on specific activity.

Excretion. Excretion of ^{14}C-radiolabeled PMOs (total radioactivity) was assessed in urine and feces collected over 336 h postdose from nine group-housed

TABLE 1

Comparison of molecular characteristics between eteplirsen, golodirsen, and casimersen

PMO	Molecular formula	Molecular weight (Daltons)	Linked subunits
Eteplirsen	$C_{364}H_{569}N_{177}O_{122}P_{30}$	10305.7	30
	Sequence of bases from the 5′ end to 3′ end: CTCCAACATCAAGGAAGATGGCATTTCTAG		
Golodirsen	$C_{305}H_{481}N_{138}O_{112}P_{25}$	8647.28	25
	Sequence of bases from the 5′ end to 3′ end: GTTGCCTCCGGTTCTGAAGGTGTTC		
Casimersen	$C_{268}H_{424}N_{124}O_{95}P_{22}$	7584.5	22
	Sequence of bases from the 5′ end to 3′ end: CAATGCCATCCTGGAGTTCCTG		

(n = 3/cage) male mice at intervals of 0–24, 24–48, 48–72, 72–120, 120–168, and 168–336 h postdose (eteplirsen) and every 24 h through 336 h (golodirsen and casimersen).

Characterization of Metabolites. Selected samples of plasma, urine, and feces were analyzed for the parent compounds and metabolites by LC-MS analysis. Samples were pooled by body sample group and collection time or interval. Plasma samples were pooled in accordance with a time-weighted scheme to generate samples representative of the AUC.

In Vitro Metabolism

Metabolism was evaluated by incubating PMOs with pooled hepatic microsomes from CD-1 male mice, Sprague–Dawley rats, NHPs, and humans, which were obtained from Celsis In Vitro Technologies (Baltimore, MD, USA). ^{14}C-radiolabeled PMOs (8 and 80 μg/mL) were incubated with microsomes (1 mg protein/mL) in the presence of 1 mM nicotinamide adenine dinucleotide phosphate (NADPH) at 37°C for 0, 30, 45, 60, and 120 minutes. Control incubations were conducted in the absence of NADPH for 0 and 120 min. Concentrations of PMOs after incubation were quantitated by LC-MS/MS, and all incubations were performed in triplicate. Metabolic activity of microsomes was confirmed by measuring phase I (7-ethoxycoumarin O-deethylase) activity (Tee et al., 1985; Bayliss et al., 1994).

Interaction With Human Cytochrome P450 Enzymes

Interaction of PMOs with human cytochrome P450 (CYP) enzymes was evaluated by incubating PMOs with resurrected cryopreserved human hepatocytes from three donors (Triangle Research Laboratories, Charlottesville, VA, USA) and comparing the effects with those of a prototypical inducer/inhibitor and a noninducer/inhibitor (with appropriate solvent controls) for each isoenzyme.

CYP Induction. PMO induction of CYP1A2, CYP2B6, and CYP3A4/5 was assessed by incubation with hepatocytes for 72 h. Prototypical inducers were omeprazole (CYP1A2), phenobarbital (CYP2B6), and rifampicin (CYP3A4/5), while flumazenil was the noninducer. Assessment of CYP enzyme induction was performed by measurement of CYP enzyme gene expression and CYP enzyme activity. Gene expression was assessed with real-time polymerase chain reaction using the comparative cycle time methodology and the TaqMan RNA-to-CT 1-Step kit (Applied Biosystems, Thermo Fisher Scientific, Waltham, MA, USA). CYP enzyme activity was evaluated by measuring the rate of production of relevant metabolites using LC-MS/MS.

CYP Inhibition. Direct (reversible) and metabolism-dependent inhibitory potential of PMOs on CYP1A2, CYP2B6, CYP2C8, CYP2C9, CYP2C19, CYP2D6, and CYP3A4/5 were characterized by incubating PMOs with pooled human hepatic microsomes from 50 individuals (25 males and 25 females) obtained from Celsis In Vitro Technologies. CYP substrates were quantified by LC-MS/MS. All sample and control incubations were performed in triplicate.

For direct inhibition, assays of CYP-selective enzyme activities were performed in the absence and presence of PMOs at eight concentrations (eteplirsen range: 0.00149–6.66 mg/mL; golodirsen range: 0.00137–6.25 mg/mL; and casimersen range: 0.00115–6.25 mg/mL). If > 50% inhibition was observed, the IC_{50} of PMO for each CYP isoenzyme was calculated and the inhibition constant (Ki) was determined, as well as the type of inhibition (e.g., competitive, noncompetitive, mechanism based).

Metabolism-dependent inhibition was assessed by adding isoenzyme-selective substrates after preincubation of eteplirsen at 0.639, 2.13, and 6.66 mg/mL; golodirsen at 0.563, 1.88, and 6.25 mg/mL; and casimersen ranging from 0.473 to 6.25 mg/mL in the presence and absence of NADPH at 37°C for 30 minutes.

Interaction With Membrane-Bound Drug Transporters

Studies were conducted to determine if eteplirsen is a substrate and/or an inhibitor of the following human transporters: bile salt export pump (BSEP), breast cancer resistance protein (BCRP), multidrug resistance protein 2 (MRP2), organic anion transporter (OAT) 1, OAT3, organic anion transporting polypeptide (OATP) 1B1, OATP1B3, organic cation transporter (OCT) 1, OCT2, and P-glycoprotein (P-gp). For golodirsen and casimersen, the following transporters were assessed: OAT1, OAT3, OCT2, OATP1B1, OATP1B3, multidrug and toxin extrusion (MATE1), MATE2-K, P-gp, BCRP, and MRP2. The concentrations of radiolabeled PMOs and transporter substrates were determined by liquid scintillation counting (LSC).

Interaction with uptake transporters (OAT1/3, OCT1/2, OATP1B1/3, MATE1, MATE2-K) was assessed by incubating PMOs with Chinese hamster ovary cells stably transfected with vector pCMV6 (eteplirsen) or human embryonic kidney 293 cells transiently transfected using vector pCMV-XL4 (golodirsen and casimersen). Assessment of eteplirsen as a substrate was evaluated by measurement of uptake of ^{14}C-eteplirsen (8 and 80 μg/mL) for 5, 15, and 30 min in the absence and presence of a known inhibitor. The inhibiting properties of ^{14}C-eteplirsen (80 and 800 μg/mL) on drug transporters was conducted in the presence and absence of a known inhibitor and substrate for 5 min (OAT1, OAT3, OCT1, and OATP1B3) or 15 min (OCT2 and OATP1B1). Evaluation of ^{14}C-golodirsen and ^{14}C-casimersen (10 and 100 μg/mL) as a substrate for each transporter was conducted in the presence of vehicle or selective inhibitor for 2 min (MATE1, MATE2-K) or 5 minutes (all other transporters). Assessment of ^{14}C-golodirsen and ^{14}C-casimersen (100 and 1000 μg/mL) as an inhibitor was conducted in the presence of vehicle and selective inhibitor. The concentrations of radiolabeled PMOs were determined by LSC.

Interactions between PMOs and the efflux transporters P-gp and BCRP were assessed using Caco-2 cells. Assessment of ^{14}C-eteplirsen (8 and 80 μg/mL) as a substrate was determined in the presence of vehicle and known inhibitor for 1, 2, 3, and 4 h and as an inhibitor (80 and 800 μg/mL) in the presence of vehicle and known inhibitor for 1 h. Determination of ^{14}C-golodirsen and ^{14}C-casimersen (10 and 100 μg/mL) as a substrate was evaluated in the presence of vehicle and known inhibitor and as an inhibitor (100 and 1000 μg/mL) in the presence of vehicle and known inhibitor at 37°C for 2 h. The concentrations of radiolabeled PMOs were determined by LSC.

For assessment of PMO interactions with the MRP2 efflux transporter, membrane vesicles prepared from baculovirus-infected insect cells (Sf9) expressing MRP2 proteins were obtained from GenoMembrane (Yokohama, Japan). For eteplirsen, the substrate assay was conducted in the presence of substrate probenecid (1000 μM), vehicle, and eteplirsen (80 and 800 μg/mL); the inhibitor assay was conducted in the presence of substrate (leukotriene C4), vehicle, and eteplirsen (80 and 800 μg/mL). For golodirsen and casimersen, the substrate assay (10 and 100 μg/mL) was conducted in the presence of vehicle or selective inhibitor (MK571 100 μM); the inhibitor assay (1000 and 1000 μg/mL) was conducted in the presence of vehicle and selective inhibitor (MK571 100 μM). The concentrations of radiolabeled substrate were determined by LSC.

For BSEP interaction assessment, inside-out human BSEP membranes derived from insect cells (Sf9) infected with a recombinant baculovirus encoding the cDNA for human BSEP were obtained from GenoMembrane. Evaluation of eteplirsen as a substrate (8 and 80 μg/mL) or as an inhibitor (80 and 800 μg/mL) of BSEP was assessed in the presence of substrate (taurocholic acid), vehicle, or inhibitor (bosentan 200 μM). The concentrations of radiolabeled substrate were determined by LSC.

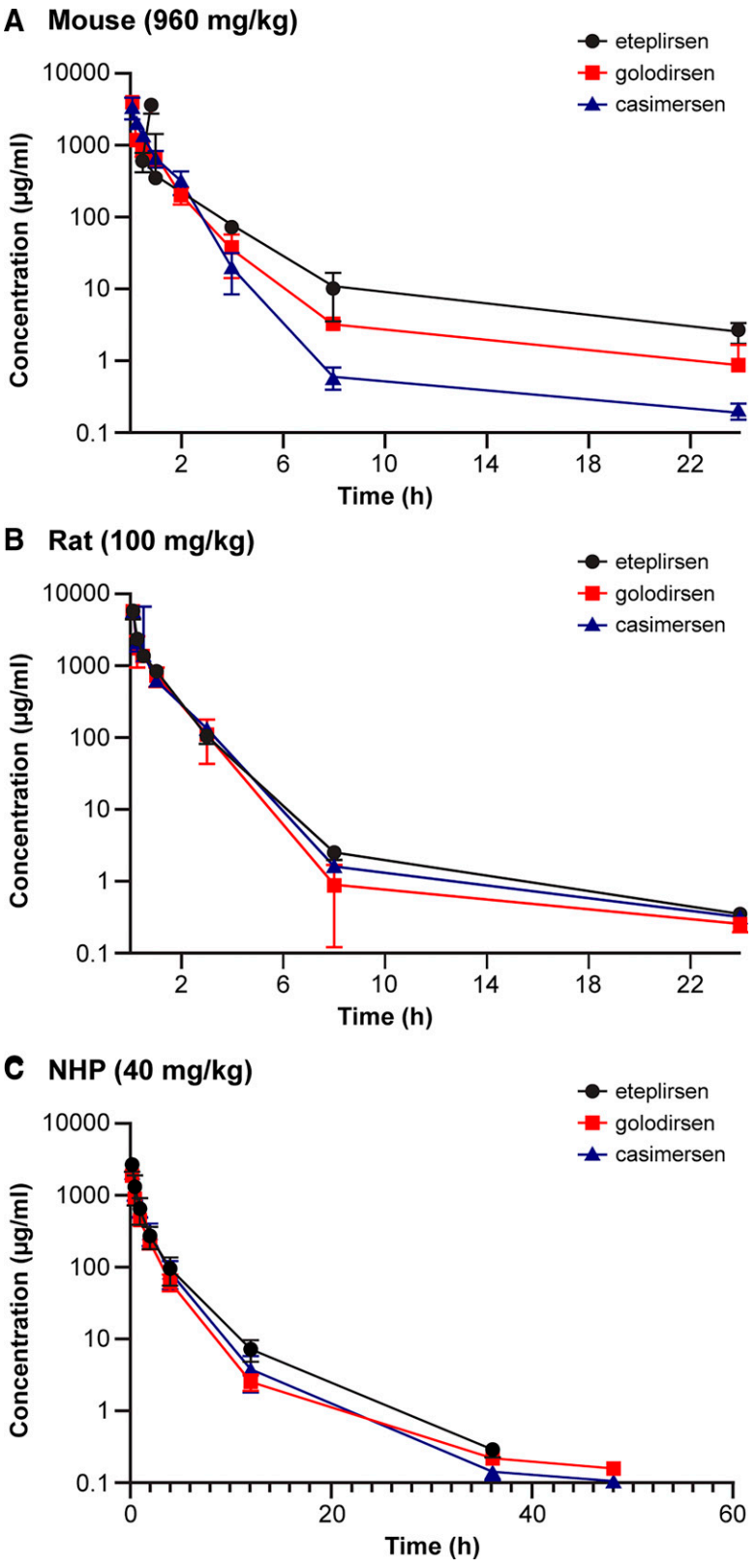

Fig. 2. Plasma concentration–time profiles of PMOs after a single dose in mice (A), rats (B), and NHPs (C). Doses shown are those considered most relevant to humans. The eteplirsen analyses were conducted in CByB6F1 mice; the golodirsen and casimersen analyses were performed in C57BL/6NCrl mice. Plots show mean ± S.D.

Statistical Analyses

For the metabolism, CYP, membrane-bound drug transporter interaction studies, plasma protein binding, and DMD mouse model studies, statistical analyses were limited to descriptive statistics such as mean, S.D., and relative S.D., where appropriate.

Results

Plasma Pharmacokinetics

After a single IV dose, the plasma concentration–time profile appeared biphasic across all three PMOs in all three species was tested,

with a rapid initial distribution phase (up to 8 h postdose in mice and rats and up to 12 h postdose in NHP) followed by a longer terminal elimination phase (up to 24 h postdose in mice and rats and up to 48 h postdose in NHP) (Fig. 2). The plasma $t_{1/2}$ [median (range), h] were 4.1 (1.0–5.8) (mouse), 2.0 (1.9–2.0) (rat), and 3.9 (1.9–4.0) (NHP) for eteplirsen; 2.1 (0.6–3.7) (mouse), 3.4 (2.7–11.6) (rat), and 8.7 (1.7–8.7) (NHP) for golodirsen; and 18.1 (15.3–20.8) (mouse), 11.9 (8.7–12.4) (rat), and 3.2 (1.4–6.1) (NHP) for casimersen (Table 2). Following IV administration of a single dose, the plasma drug exposure of the three PMOs increased with dose in mice (12–960 mg/kg), rats (100–900 mg/kg), and NHPs (5–320 mg/kg) (Fig. 3, A–C).

Plasma Protein Binding

The average percentage of plasma protein binding in mouse, rat, NHP, and human plasma was low for all three PMOs and was largely concentration independent at concentrations assessed (8, 24, 80, 240, and 800 μg/mL), with an unbound fraction > 60% in the species tested (Table 3). Mean (S.D.) unbound plasma protein was 78.4% (3.46) (mouse), 92.3% (6.40) (rat), and 96.3% (3.08) (NHP) for eteplirsen; 63.8% (6.21) (mouse), 79.9% (6.10) (rat), and 64.3% (1.47) (NHP) for golodirsen; and 82.6% (11.3) (mouse), 78.9% (8.69) (rat), and 86.9% (8.49) (NHP) for casimersen. In human plasma, mean (S.D.) unbound protein was 86.7% (4.14) for eteplirsen, 62.8% (2.43) for golodirsen, and 78.8% (10.1) for casimersen.

Distribution and Excretion in the DMD Mouse Model

PK parameters in blood and plasma after a single injection of radiolabeled PMOs in *mdx* mice are shown in Table 4. Blood-to-plasma concentration ratios at time of maximum observed concentration (0.083 h) were 0.547 (eteplirsen), 0.622 (golodirsen), and 0.633 (casimersen), indicating no preferential binding of radioactivity or drug sequestration to the cellular component of blood. PK data were consistent with the findings of the nonradiolabeled studies (Supplemental Table 1).

Tissue Biodistribution. After a single injection, the concentration–time profiles of all three ^{14}C-PMOs appeared to be similar in plasma and in each of the tissues tested (selected tissues shown in Fig. 4; additional tissues shown in Supplemental Fig. 1). The highest levels of tissue exposure were identified in the kidney for all three PMOs. Extensive distribution of all three PMOs was observed in the target skeletal muscle tissues assessed (Fig. 4, Supplemental Fig. 1). Maximum concentrations of ^{14}C-PMOs were reached at 0.25 h postdose in all eight tissues examined for all three PMOs, with the exception of golodirsen in the brain (peak concentration at 1 h postdose). Tissue-to-plasma exposure ratios (AUC from time zero to the last measurable concentration) ranged from 0.9–1.4 in heart, 1.6–1.9 in quadriceps, and 49–103 in kidney (Fig. 5), indicating increased drug accumulation in the kidney. All skeletal muscle tissues analyzed had measurable concentrations of ^{14}C-PMO at 144 h postdose (time of last measurable concentration) for all three PMOs. In plasma, time of last measurable concentration values were 4, 8, and 24 h postdose for casimersen, golodirsen, and eteplirsen, respectively.

TABLE 2

Half-life across all PMO dose levels

PMO	Mouse	Rat	NHP
Eteplirsen	4.1 (1.0–5.8)	2.0 (1.9–2.0)	3.9 (1.9–4.0)
Golodirsen	2.1 (0.6–3.7)	3.4 (2.7–11.6)	8.7 (1.7–8.7)
Casimersen	18.1 (15.3–20.8)	11.9 (8.7–12.4)	3.2 (1.4–6.1)

Values are median (range), h.
Mouse: 12, 120, or 960 mg/kg for golodirsen and casimersen; 100, 300, 600, 960 mg/kg for eteplirsen.
Rat: 100, 300, or 900 mg/kg. NHP: 5, 40, or 320 mg/kg.

In whole-body autoradiographic analyses, the highest levels of radioactivity were found in urine and kidney, suggesting a predominantly renal route of excretion.

Excretion. The mean total recovery of the administered dose following a single IV administration of ^{14}C-PMO through 336 h postdose was 83.2 ± 2.02% for eteplirsen, 93.1 ± 0.50% for golodirsen, and 90.3 ± 4.26% for casimersen. Renal excretion was the primary route of elimination for all three PMOs, with fecal elimination involved to a lesser extent (Fig. 6). The mean percentage of radioactive dose recovered in the urine in the first 24 h for eteplirsen was 28.3%, and mean percentages of radioactive dose excreted by 336 h postdose were 42.6% in urine and 15.9% in feces. Additional recoveries of the radioactive eteplirsen dose were found in the carcass (1.1%), cage rinse (17.4%), and cage wash and cage wipes (10.2%). The majority of radioactive dose in the urine was recovered in the first 24 h for golodirsen (71.2%) and casimersen (66.5%). Mean percentages of radioactive dose excreted by 336 h postdose were 74.9% in urine and 9.6% in feces for golodirsen and 68.9% in urine and 12.5% in feces for casimersen. Excretion of radioactivity was essentially complete for all three PMOs at 336 h postdose.

Characterization of Metabolites. Radiochemical and LC-MS analysis of plasma, urine, and feces indicated that golodirsen and casimersen were metabolically stable and excreted primarily as unchanged test articles in urine and feces (assessment not conducted for eteplirsen).

In Vitro Metabolism

All three PMOs were chemically stable in mouse, rat, NHP, and human liver microsomes under the study conditions, with no difference versus controls, showing a lack of substantive time- and NADPH-dependent metabolism (Supplemental Table 2). This is consistent with the metabolic stability observed in *mdx* mice.

Interactions With Cytochrome P450 Enzymes

CYP Induction. Eteplirsen did not induce CYP2B6 or CYP3A4 enzymes. mRNA data suggested CYP1A2 induction for donors 2 and 3 only, while enzyme activity assessment suggested induction of CYP1A2 in all three donors. Induction of CYP1A2 mRNA by eteplirsen at 6.66 mg/mL was 2.51-, 6.69-, and 5.41-fold, and CYP1A2 enzyme activity was 4.07-, 7.51-, and 5.28-fold. However, the levels of induction were generally much lower than that of the prototypical inducer omeprazole in all three donors. Induction of CYP1A2 mRNA by omeprazole 50 μM was 63.7-, 90.5-, and 46.5-fold, and CYP1A2 enzyme activity was 35.5-, 21.7-, and 57.6-fold. Also, maximum plasma concentrations (C_{max}) of eteplirsen (30 mg/kg, once weekly) in DMD patients are substantially lower (0.06–0.08 mg/mL) (Mercuri et al., 2023). For golodirsen, there was no induction of CYP2B6 and CYP3A4. A low level of induction of CYP1A2 enzyme activity was observed only at the highest concentration tested (6.25 mg/mL) and was not supported by induction of CYP1A2 mRNA levels. In addition, the mean plasma C_{max} of golodirsen at a weekly dose of 30 mg/kg is much lower (0.05 mg/mL (Frank et al., 2020). Therefore, low induction of CYP1A2 by golodirsen is unlikely to result in clinically relevant drug–drug interactions. Similarly for casimersen, no induction of CYP1A2, CYP2B6, and CYP3A4 enzymes was observed.

CYP Inhibition. No metabolism-dependent inhibition was observed by eteplirsen, since similar microsomal CYP enzyme activity results with eteplirsen were observed with or without 30-min preincubation with NAPDH. Also, no direct inhibition by eteplirsen at a level > 50% was observed for CYP2B6, CYP2C8, CYP2D6, or CYP3A4/5 at concentrations up to 6.66 mg/mL. Observed direct inhibition by eteplirsen at 6.66 mg/mL was 13.1% for CYP2B6 (thioTEPA at 100 μM inhibited CYP2B6 activity by 82.7%), 14.4% for CYP2C8 (montelukast at

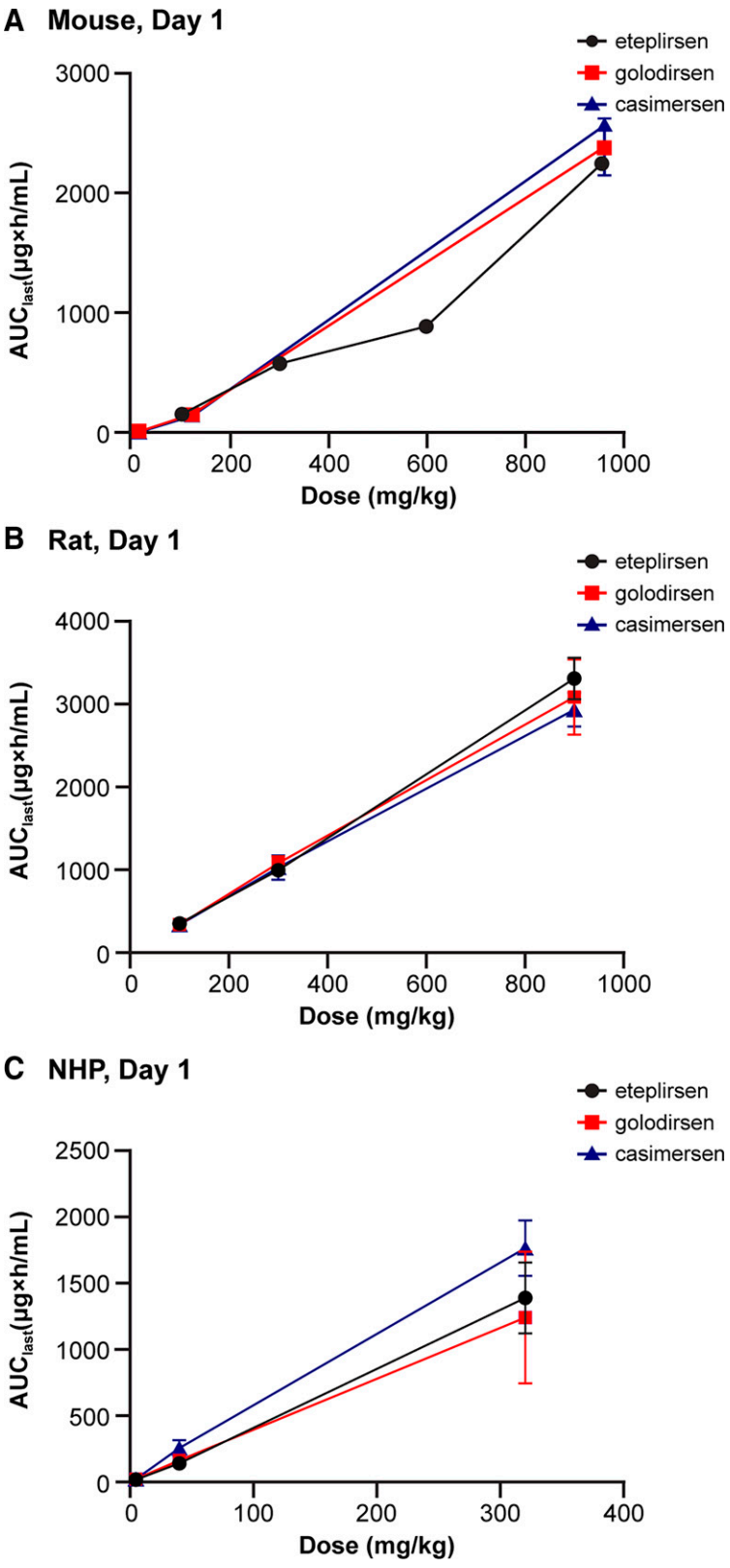

Fig. 3. Plasma PK exposures of PMOs after a single dose in mice (A), rats (B), and NHPs (C). All samples were collected immediately after single doses of 5, 40, and 320 mg/kg in NHPs; 100, 300, and 900 mg/kg in rats; and 12, 120, and 960 mg/kg (golodirsen and casimersen) in C57BL/6NCrl mice or 100, 300, 600, and 960 mg/kg (eteplirsen) in CByB6F1 mice. Plots show mean ± S.D. AUC_{last}, area under the concentration–time curve from time zero to the last measurable concentration.

0.1 μM inhibited CYP2C8 activity by 64.5%), 10.6% for CYP2D6 (quinidine at 0.3 μM inhibited CYP2D6 activity by 79.6%), and 30.8% for CYP3A4/5 (ketoconazole at 0.2 μM inhibited CYP3A4/5 activity by 88.7%). Inhibition of CYP2C9 and CYP2C19 by eteplirsen was determined to be competitive (IC_{50} and Ki values are shown in Supplemental Table 3). For CYP1A2, the Ki value was not approximately half that of the IC_{50} value (characteristic for competitive inhibition) (Supplemental Table 3), therefore mixed or noncompetitive inhibition of CYP1A2 activity could not be ruled out. For golodirsen, no metabolism-dependent or direct inhibition at a level > 50% was

TABLE 3

Mean percentage of unbound plasma protein (S.D.) across PMO concentrations tested

PMO	Mouse	Rat	NHP	Human plasma
Eteplirsen	78.4 (3.46)	92.3 (6.40)	96.3 (3.08)	86.7 (4.14)
Golodirsen	63.8 (6.21)	79.9 (6.10)	64.3 (1.47)	62.8 (2.43)
Casimersen	82.6 (11.3)	78.9 (8.69)	86.9 (8.49)	78.8 (10.1)

Values are mean of percentage of unbound fraction. Plasma protein binding was assessed at PMO concentrations of 8, 24, 80, 240, and 800 μg/mL.

observed at concentrations up to 6.25 mg/mL. For casimersen, no metabolism-dependent inhibition was observed, and no direct inhibition at a level > 50% was observed for CYP1A2, CYP2B6, CYP2C8, or CYP2D6 concentrations up to 5.89 mg/mL. Inhibition by casimersen was competitive for CYP2C9, CYP2C19, and CYP3A4/5 (IC_{50} and Ki values are shown in Supplemental Table 3).

Interaction With Membrane-Bound Drug Transporters

None of the PMOs were identified to be substrates or inhibitors of the tested human transporters at clinically relevant concentrations, i.e., plasma C_{max} in DMD patients at the clinically approved weekly dose of 30 mg/kg are 0.06 to 0.08 mg/mL for eteplirsen (Mercuri et al., 2023), 0.05 mg/mL for golodirsen (Frank et al., 2020), and 0.1 mg/mL for casimersen (Wagner et al., 2021). Eteplirsen showed weak inhibition of OCT1 and OATP1B1. Golodirsen showed weak inhibition of substrate uptake by OATP1B3 and MATE2-K when tested at 100 and 1000 μg/mL, with estimated IC_{50} values > 1000 μg/mL. Casimersen weakly inhibited MATE1; the IC_{50} value was not determined but estimated to be > 1000 μg/mL.

Discussion

These findings provide a comprehensive nonclinical PK evaluation of eteplirsen, golodirsen, and casimersen, critical for the clinical development and clinical pharmacology evaluation of this novel drug class. Findings from both in vivo and in vitro studies demonstrated that key ADME and DMPK features were broadly consistent across the three PMOs tested. Single IV bolus administration of the three PMOs at similar doses (including the clinically approved dose of 30 mg/kg in NHP) resulted in similar plasma PK exposures across all three PMOs in mouse, rat, and NHP. Across a wide dose range inclusive of the therapeutic dose for DMD at 30 mg/kg, all three PMOs exhibited predominantly linear plasma PK and dose-proportional increases in plasma exposure. Plasma protein binding of all three PMOs was low in all species tested, including human plasma, and was largely independent of PMO concentration across 8 to 800 μg/mL inclusive of the clinical exposures at the therapeutic dose, allowing for extrapolation and comparisons across PMOs. Extensive biodistribution was observed in the target muscle tissues, supporting effective target engagement and downstream biological efficacy.

There was no evidence for hepatic metabolism of the PMOs in vitro (mouse, rat, monkey, and human hepatic microsomes) or in vivo (golodirsen and casimersen in the DMD mouse model), demonstrating metabolic stability. In in vitro studies, none of the PMOs were identified as substrates, inhibitors, or inducers of the human CYP enzymes or membrane drug transporters tested at clinically relevant concentrations (Patel et al., 2023). At high eteplirsen concentrations of 6.66 mg/mL (well above the clinical plasma C_{max} of 0.08 mg/mL (Mercuri et al., 2023), modest CYP1A2 induction was observed in human cryopreserved hepatocytes (compared with the prototypical CYP1A2 inducer omeprazole). The mechanism of CYP1A2 induction remains uncertain, as CYP1A2 induction is regulated by the ligand-activated aryl hydrocarbon receptor (AhR), which resides in the cytosol. As such, PMOs like eteplirsen are generally taken up the cell by endocytosis (Takakusa et al., 2023) and limited intracellular interaction is expected between eteplirsen and cytosolic AhR. In addition, AhR inducers are typically small molecules (e.g., kynurenine, dioxin, omeprazole), which makes direct binding to AhR by a larger PMO molecule like eteplirsen unlikely. An indirect mechanism through modulation of CYP1A2 mRNA cannot be ruled out, but scientific evidence for this is lacking. At the highest tested in vitro concentration of 6.66 mg/mL, IC_{50} and Ki values suggest competitive CYP2C9 and CYP2C19 inhibition by eteplirsen in human liver microsomes (HLMs). The exact mechanism, however, requires confirmation as typically smaller molecules bind to the active site of CYP2C9/19 enzymes (Flockhart, 2024). Also, HLMs may not have been the most clinically relevant test system to evaluate the CYP inhibitory potential of PMOs. For example, phosphorothioate antisense oligonucleotides were found to be potent inhibitors of CYP and UGT enzymes in HLMs, but little to no inhibition was found in cryopreserved human hepatocytes (Kazmi et al., 2018). Cellular uptake of these oligonucleotides by endocytosis sequestering them from CYP and UGT enzymes could be one of the reasons for the lack of significant inhibitory effects in hepatocytes. Based on this background, CYP2C9/19 inhibition by eteplirsen is unlikely in human cryopreserved hepatocytes and in patients. Moreover, the inhibitory concentrations in vitro are not likely to be reached clinically based on the substantially lower C_{max} of

TABLE 4

PK parameters in blood and plasma for PMOs after a single IV administration of 120 mg/kg of ^{14}C radiolabeled PMO in a DMD mouse model

PMO	Matrix	C_0, ng eq/g	C_{max}, ng eq/g	T_{max}, h	$t_{1/2}$, h	$AUC_{(0-last)}$, ng eq×h/g	$AUC_{(0-inf)}$, ng eq×h/g	CL, g/h/kg	V_{ss}, g/kg	Blood: plasma concentration ratio[a]
Eteplirsen	Blood	1,380,000	xx	xx	NC	185,000	NA	NA	NA	0.547
	Plasma	2,490,000	xx	xx	6.03	344,000	345,000	348[b]	175[c]	
Golodirsen	Blood	677,000	339,000	0.0830	1.46	117,000	117,000	1,020	325	0.622
	Plasma	1,130,000	544,000	0.0830	NC[d]	182,000	NC	NC	NC	
Casimersen	Blood	782,000	363,000	0.0830	0.291	123,000	124,000	971	237	0.633
	Plasma	1,230,000	576,000	0.0830	0.438	196,000	196,000	613	155	

AUC(0–inf), AUC from time zero to infinity; AUC(0–last), AUC from time zero to the last measurable concentration; C_0, extrapolated concentration at time zero; CL, total body clearance; eq, equivalents; NA, not applicable; NC, not calculated; T_{max}, time of maximum observed concentration; V_{ss}, volume of distribution at steady state.

[a]Samples were collected at 0.083 h (equivalent to T_{max}).

[b]Units are mL/h/kg.

[c]Volume of distribution (Vd); units are mL/kg.

[d]For golodirsen, the $t_{1/2}$ in plasma was not calculated due to the inability to characterize the elimination phase in this matrix.

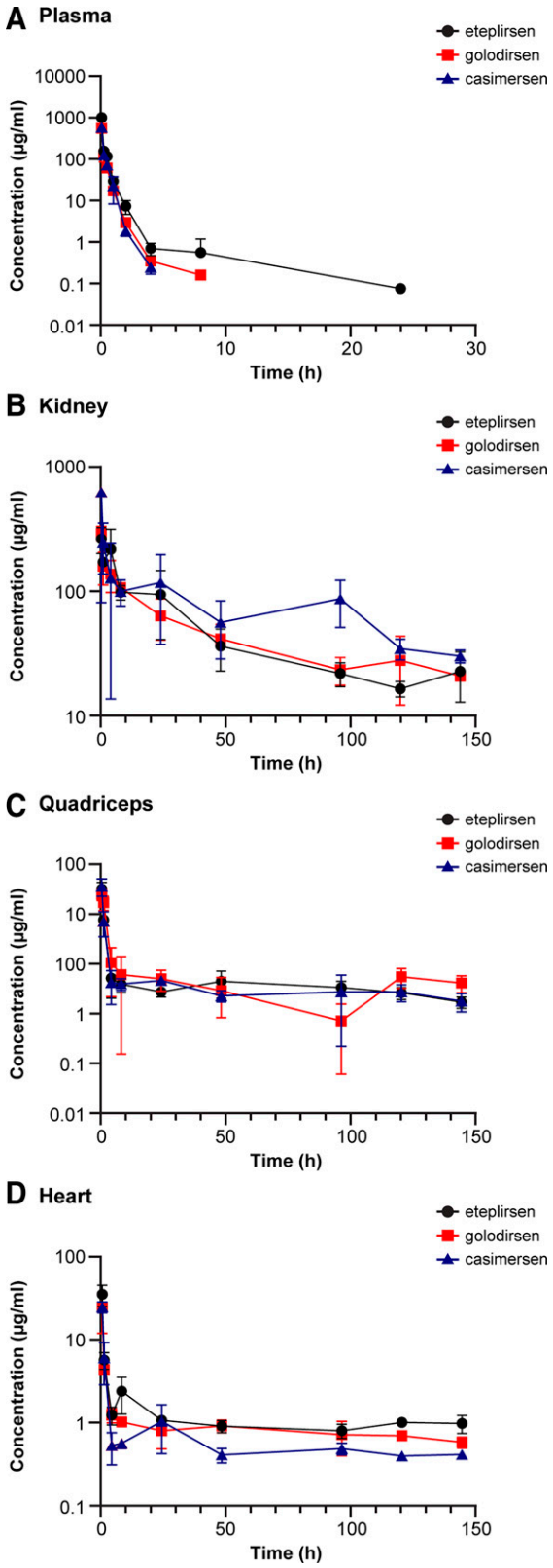

Fig. 4. Distribution of ^{14}C-PMOs in plasma (A), kidney (B), and quadriceps (C) after a single injection (120 mg/kg) in a DMD mouse model. Plots show mean ± S.D.

eteplirsen in DMD patients at the clinically approved weekly dose of 30 mg/kg.

The three PMOs were predominantly excreted renally and radiolabeled ADME studies in mice showed that recoveries of ^{14}C-labeled

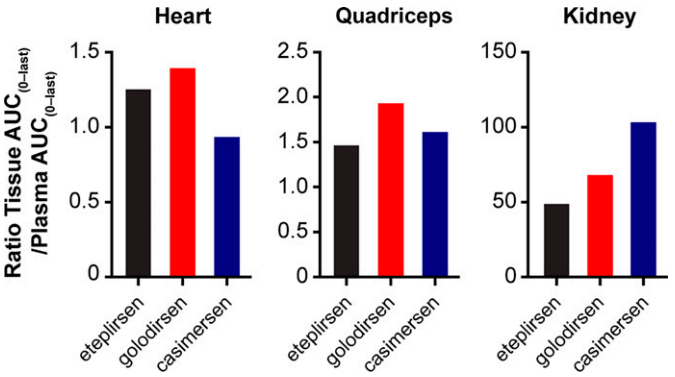

Fig. 5. Tissue-to-plasma exposure ratios after a single IV administration of 120 mg/kg ^{14}C-casimersen, ^{14}C-eteplirsen, or ^{14}C-golodirsen in a DMD mouse model. T_{last} in the evaluated tissues was 144 h postdose. In plasma, t_{last} values were 4, 8, and 24 h postdose for casimersen, golodirsen, and eteplirsen, respectively. $AUC_{(0–last)}$, area under the concentration–time curve from time zero to the last measurable concentration; t_{last}, time of last measurable concentration.

PMOs in feces were similar (Fig. 5B). For eteplirsen, however, lower urinary recovery was observed (Fig. 5A), which could be caused by urinary residues in the cages that could not be removed at the scheduled collection as evidenced by high recoveries in cage rinse (17.4%) and cage wash and cage wipes (10.2%). Similar urinary recoveries across

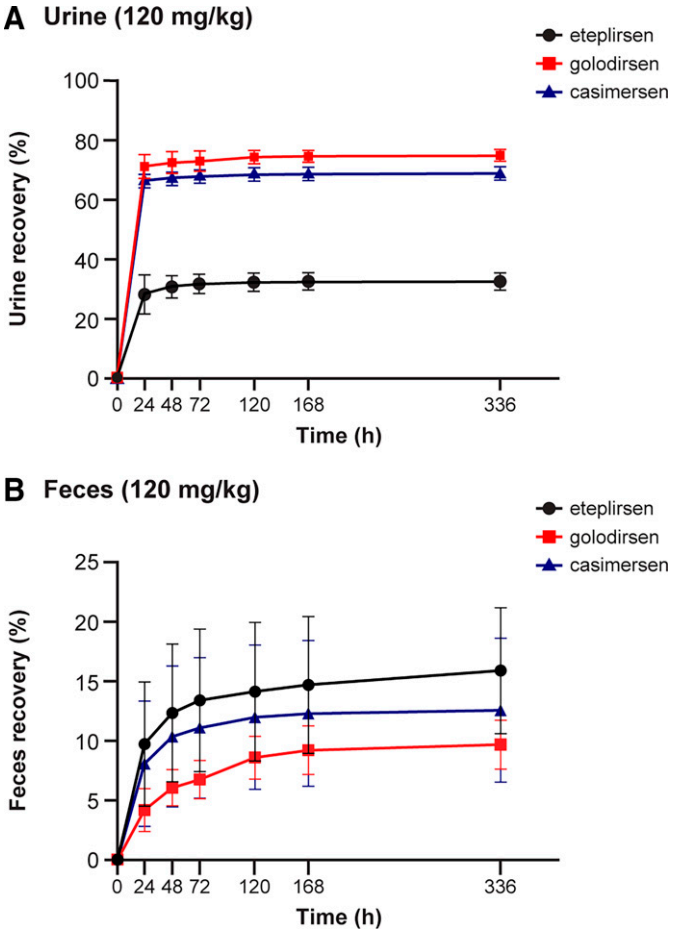

Fig. 6. Percentage recovery of ^{14}C-PMO total injected radioactivity in urine (A) and feces (B) after a single IV bolus injection in a DMD mouse model. One of the three groups of mice in the eteplirsen study had a different excretion profile than the other two groups. Fecal excretion was higher than urinary excretion in this group. These results could have been the result of urinary contamination of feces. This group was excluded from the eteplirsen dataset for calculation of the mean.

the three PMOs were found in a clinical radiolabeled study (Patel et al., 2023).Taken together, these findings provide favorable and predictable ADME and DMPK characteristics across PMOs and suggest minimal liability for drug–drug interactions following PMO therapy.

In phase 1 studies of single-dose ^{14}C-labeled PMOs in healthy volunteers, eteplirsen had an effective half-life of 5.31 h, and golodirsen and casimersen had half-lives of 6.35 h and 5.10 h, respectively (Patel et al., 2023). The variability in half-life between PMOs across species (mice, rats, NHP) after a single dose could be attributed to variability in sampling times, which may impact how long the PMO is detected in plasma and what data may be used for determination of a $t_{1/2}$. In comparison with eteplirsen sample collection timepoints, additional earlier (0.25, 2 h) and later (36, 48 h) timepoints in mice and later timepoints in rats (36, 48 h) and NHP (48 h) were added for golodirsen and casimersen.

A possible limitation of the plasma exposure data may be the use of a different mouse strain for assessment of eteplirsen, thus precluding direct comparison of eteplirsen exposure with golodirsen and casimersen in this manuscript; however, exposure was generally similar, with dose-proportional or greater-than-dose-proportional increases in exposure for all three PMOs. Data collected in healthy volunteers and patients with DMD demonstrated consistent exposures between eteplirsen, golodirsen, and casimersen at the approved weight-based dosing (30 mg/kg), and plasma exposures increased proportionally with dose, suggesting linear PK for all three PMOs. Another limitation was the lack of metabolite profiling of ^{14}C-eteplirsen in the distribution and elimination study in *mdx* mice. However, based on the similar in vitro metabolism results and similar PK profiles across species for the three PMOs, it seems reasonable to assume that eteplirsen does not undergo extensive metabolism in vivo. In studies in healthy volunteers and patients with DMD, eteplirsen (like golodirsen and casimersen) was metabolically stable, with no metabolites detected in systemic circulation, supporting the findings with golodirsen and casimersen described herein (Vyondys 53, 2021; Exondys 51, 2022; Amondys 45, 2023).

Structurally, casimersen, eteplirsen, and golodirsen are all uncharged and share the same chemistry backbone (Fig. 1) while differing in the number morpholino subunits (Table 1). The structural similarity of these PMOs provides preliminary evidence that a platform approach may be considered for these drugs based on the recently published FDA draft guidance "Platform Technology Designation Program for Drug Development" (FDA, 2024). Drug discovery platform technologies facilitate efficiency, quality, and innovation in drug product development (Crooke et al., 2018; Bennett et al., 2019). Platforms group drug development technologies together and leverage accrued knowledge for existing molecule technology to fast-track the development of novel drug candidates. Incorporation of new data from successive generations of molecule technology enables continuous improvement and robustness of the platform. Further, a platform approach may benefit drug development for rare disease subtypes that have few patients available to participate in clinical trials. Leveraging collective data for a drug class may facilitate further drug development opportunities, thereby allowing treatments for such patient populations to become accessible.

Overall, these findings provide evidence for the concept that PMOs represent a treatment class, where the consistent structural, ADME, and DMPK characteristics may support a platform approach in understanding the kinetic and dynamic behavior of PMOs.

Acknowledgments

The authors thank Jason W. Boggs for his contributions to data acquisition, analysis, and interpretation. Mohammad Shadid, John Hadcock, and Jianbo Zhang are acknowledged for conducting the nonclinical studies. Editorial support was provided by Paraskevi Briassouli, of Eloquent Scientific Solutions, and was funded by Sarepta Therapeutics, Inc.

Data Availability

Qualified researchers may request access to the data that support the findings of this study from Sarepta Therapeutics, Inc. by contacting medinfo@sarepta.com.

Authorship Contributions

Participated in research design: Mukashyaka, Patel, Rodino-Klapac, East.

Performed data analysis: Goey, Mukashyaka, Patel.

Wrote or contributed to the writing of the manuscript: Goey, Mukashyaka, Patel, Rodino-Klapac, East.

References

Aartsma-Rus A, Fokkema I, Verschuuren J, Ginjaar I, van Deutekom J, van Ommen G-J, and den Dunnen JT (2009) Theoretic applicability of antisense-mediated exon skipping for Duchenne muscular dystrophy mutations. *Hum Mutat* **30:**293–299.

Amondys 45 (2023) (Casimersen) injection, for intravenous use. Prescribing information. Cambridge, MA: Sarepta Therapeutics, Inc.

Bayliss MK, Bell JA, Wilson K, and Park GR (1994) 7-Ethoxycoumarin O-deethylase kinetics in isolated rat, dog and human hepatocyte suspensions. *Xenobiotica* **24:**231–241.

Bello L, Gordish-Dressman H, Morgenroth LP, Henricson EK, Duong T, Hoffman EP, Cnaan A, McDonald CM, and CINRG Investigators (2015) Prednisone/prednisolone and deflazacort regimens in the CINRG Duchenne Natural History Study. *Neurology* **85:**1048–1055.

Bennett CF, Krainer AR, and Cleveland DW (2019) Antisense oligonucleotide therapies for neurodegenerative diseases. *Annu Rev Neurosci* **42:**385–406.

Bulfield G, Siller WG, Wight PA, and Moore KJ (1984) X chromosome-linked muscular dystrophy (mdx) in the mouse. *Proc Natl Acad Sci U S A* **81:**1189–1192.

Bushby K, Finkel R, Birnkrant DJ, Case LE, Clemens PR, Cripe L, Kaul A, Kinnett K, McDonald C, Pandya S, et al. DMD Care Considerations Working Group (2010) Diagnosis and management of Duchenne muscular dystrophy, part 1: diagnosis, and pharmacological and psychosocial management. *Lancet Neurol* **9:**77–93.

Carver MP, Charleston JS, Shanks C, Zhang J, Mense M, Sharma AK, Kaur H, and Sazani P (2016) Toxicological characterization of exon skipping phosphorodiamidate morpholino oligomers (PMOs) in non-human primates. *J Neuromuscul Dis* **3:**381–393.

Clemens PR, Rao VK, Connolly AM, Harper AD, Mah JK, Smith EC, McDonald CM, Zaidman CM, Morgenroth LP, Osaki H, et al. CINRG DNHS Investigators (2020) Safety, tolerability, and efficacy of viltolarsen in boys with Duchenne muscular dystrophy amenable to exon 53 skipping: a phase 2 randomized clinical trial. *JAMA Neurol* **77:**982–991.

Crooke ST, Witztum JL, Bennett CF, and Baker BF (2018) RNA-targeted therapeutics. *Cell Metab* **27:**714–739.

Duan D, Goemans N, Takeda S, Mercuri E, and Aartsma-Rus A (2021) Duchenne muscular dystrophy. *Nat Rev Dis Primers* **7:**13.

Elevidys (2024) (Delandistrogene moxeparvovec-rokl) suspension, for intravenous infusion Prescribing information. Cambridge, MA: Sarepta Therapeutics, Inc.

Exondys 51 (2022) (Eteplirsen) injection, for intravenous use. Prescribing information. Cambridge, MA: Sarepta Therapeutics, Inc.

Flockhart DA (2024) *Drug interactions Flockhart table.* Indianapolis, IN: Indiana University.

Food and Drug Administration (2024) Platform technology designation program for drug development guidance for industry. Silver Spring, MD: Food and Drug Administration.

Frank DE, Schnell FJ, Akana C, El-Husayni SH, Desjardins CA, Morgan J, Charleston JS, Sardone V, Domingos J, Dickson G, et al. SKIP-NMD Study Group (2020) Increased dystrophin production with golodirsen in patients with Duchenne muscular dystrophy. *Neurology* **94:**e2270–e2282.

Guglieri M, Bushby K, McDermott MP, Hart KA, Tawil R, Martens WB, Herr BE, McColl E, Speed C, Wilkinson J, et al. FOR-DMD Investigators of the Muscle Study Group (2022) Effect of different corticosteroid dosing regimens on clinical outcomes in boys with Duchenne muscular dystrophy: a randomized clinical trial. *JAMA* **327:**1456–1468.

Iff J, Done N, Tuttle E, Zhong Y, Wei F, Darras BT, McDonald CM, Mercuri E, and Muntoni F (2024) Survival among patients receiving eteplirsen for up to 8 years for the treatment of Duchenne muscular dystrophy and contextualization with natural history controls. *Muscle Nerve* **70:**60–70.

Kazmi F, Yerino P, McCoy C, Parkinson A, Buckley DB, and Ogilvie BW (2018) An assessment of the in vitro inhibition of cytochrome P450 enzymes, UDP-glucuronosyltransferases, and transporters by phosphodiester- or phosphorothioate-linked oligonucleotides. *Drug Metab Dispos* **46:**1066–1074.

Kole R, Krainer AR, and Altman S (2012) RNA therapeutics: beyond RNA interference and antisense oligonucleotides. *Nat Rev Drug Discov* **11:**125–140.

Landfeldt E, Edström J, Buccella F, Kirschner J, and Lochmüller H (2018) Duchenne muscular dystrophy and caregiver burden: a systematic review. *Dev Med Child Neurol* **60:**987–996.

Mendell JR, Rodino-Klapac LR, Sahenk Z, Roush K, Bird L, Lowes LP, Alfano L, Gomez AM, Lewis S, Kota J, et al. Eteplirsen Study Group (2013) Eteplirsen for the treatment of Duchenne muscular dystrophy. *Ann Neurol* **74:**637–647.

Mendell JR, Goemans N, Lowes LP, Alfano LN, Berry K, Shao J, Kaye EM, and Mercuri E (2016) Eteplirsen Study Group and Telethon Foundation DMD Italian Network. Longitudinal effect of eteplirsen versus historical control on ambulation in Duchenne muscular dystrophy. *Ann Neurol* **79:**257–271.

Mendell JR, Khan N, Sha N, Eliopoulos H, McDonald CM, Goemans N, Mercuri E, Lowes LP, and Alfano LN. Eteplirsen Study Group. (2021) Comparison of long-term ambulatory function in patients with Duchenne muscular dystrophy treated with eteplirsen and matched natural history controls. *J Neuromuscul Dis* **8:**469–479.

Mercuri E, Seferian AM, Servais L, Deconinck N, Stevenson H, Ni X, Zhang W, East L, Yonren S, and Muntoni F. 4658-102 Study Group (2023) Safety, tolerability and pharmacokinetics of eteplirsen in young boys aged 6–48 months with Duchenne muscular dystrophy amenable to exon 51 skipping. *Neuromuscul Disord* **33:**476–483.

Nascimento Osorio A, Medina Cantillo J, Camacho Salas A, Madruga Garrido M, and Vilchez Padilla JJ (2019) Consensus on the diagnosis, treatment and follow-up of patients with Duchenne muscular dystrophy. *Neurologia (Engl Ed)* **34:**469–481.

Patel Y, Mukashyaka C, Yocum N, Elkins J, Rodino-Klapac LR, and East L (2023) Eteplirsen, golodirsen, and casimersen show consistent clinical pharmacology properties for the treatment of Duchenne muscular dystrophy. Presented at American Society for Clinical Pharmacology & Therapeutics 2023 Annual Meeting, March 22-24, 2023, Atlanta, GA.

Popplewell LJ, Trollet C, Dickson G, and Graham IR (2009) Design of phosphorodiamidate morpholino oligomers (PMOs) for the induction of exon skipping of the human DMD gene. *Mol Ther* **17:**554–561.

Ryder-Cook AS, Sicinski P, Thomas K, Davies KE, Worton RG, Barnard EA, Darlison MG, and Barnard PJ (1988) Localization of the mdx mutation within the mouse dystrophin gene. *EMBO J* **7:**3017–3021.

Sazani P, Weller DL, and Shrewsbury SB (2010) Safety pharmacology and genotoxicity evaluation of AVI-4658. *Int J Toxicol* **29:**143–156.

Sazani P, Ness KPV, Weller DL, Poage D, Nelson K, and Shrewsbury ASB (2011a) Chemical and mechanistic toxicology evaluation of exon skipping phosphorodiamidate morpholino oligomers in mdx mice. *Int J Toxicol* **30:**322–333.

Sazani P, Ness KPV, Weller DL, Poage DW, Palyada K, and Shrewsbury SB (2011b) Repeat-dose toxicology evaluation in cynomolgus monkeys of AVI-4658, a phosphorodiamidate morpholino oligomer (PMO) drug for the treatment of Duchenne muscular dystrophy. *Int J Toxicol* **30:**313–321.

Servais L, Mercuri E, Straub V, Guglieri M, Seferian AM, Scoto M, Leone D, Koenig E, Khan N, Dugar A, et al. SKIP-NMD Study Group (2022) Long-term safety and efficacy data of golodirsen in ambulatory patients with Duchenne muscular dystrophy amenable to exon 53 skipping: a first-in-human, multicenter, two-part, open-label, phase 1/2 trial. *Nucleic Acid Ther* **32:**29–39.

Sicinski P, Geng Y, Ryder-Cook AS, Barnard EA, Darlison MG, and Barnard PJ (1989) The molecular basis of muscular dystrophy in the mdx mouse: a point mutation. *Science* **244:**1578–1580.

Takakusa H, Iwazaki N, Nishikawa M, Yoshida T, Obika S, and Inoue T (2023) Drug metabolism and pharmacokinetics of antisense oligonucleotide therapeutics: typical profiles, evaluation approaches, and points to consider compared with small molecule drugs. *Nucleic Acid Ther* **33:**83–94.

Tee LB, Seddon T, Boobis AR, and Davies DS (1985) Drug metabolising activity of freshly isolated human hepatocytes. *Br J Clin Pharmacol* **19:**279–294.

Viltepso (2021) (Viltolarsen) injection, for intravenous use. Prescribing information. Paramus, NJ: NS Pharma, Inc.

Vyondys 53 (2021) (Golodirsen) injection, for intravenous use. Prescribing information. Cambridge, MA: Sarepta Therapeutics, Inc.

Wagner KR, Kuntz NL, Koenig E, East L, Upadhyay S, Han B, and Shieh PB (2021) Safety, tolerability, and pharmacokinetics of casimersen in patients with Duchenne muscular dystrophy amenable to exon 45 skipping: a randomized, double-blind, placebo-controlled, dose-titration trial. *Muscle Nerve* **64:**285–292.

Address correspondence to: Andrew Goey, Sarepta Therapeutics, Inc., 215 First Street, Cambridge, MA 02142. E-mail: agoey@sarepta.com